The Cardiovascular Impact and Genetics of Pericardial Adiposity

Supplementary Information

Table of Contents

Supplementary Methods

Fine-tuning of the deep learning model

All four-chamber images were resized to 168 x 208 pixels and normalized using mean and standard deviation estimates from ImageNet[1]. The model was fine-tuned with a batch size of four. Augmentations with rotations up to 90 degrees were applied. Gradient clipping was used to limit the size of the gradients. The learning rate was chosen as $1x10^{-4}$ based on the learning rate finder and the model was trained for 50 cycles while monitoring the Dice score. We applied the fine-tuned model to randomly selected four-chamber CMR images from all remaining 45,263 UKB participants after excluding participants in the training, validation and test sets.

Additional quality control for CMR images

A small proportion of the UK Biobank four-chamber CMR images were misaligned (not true four-chamber images) or of poor quality e.g. due to imaging artifacts. To exclude these images from final analyses, we first manually annotated the four cardiac chambers (left ventricle, left atrium, right ventricle, right atrium) in the same training data that was used for PAT model training. The deep learning model based on Resnet50 was fine-tuned with additional labels for the four cardiac chambers and used to infer the segmentation of the cardiac chambers in addition to PAT[2]. We excluded any images in which any of the cardiac chambers was predicted to have an area less than $5cm^2$.

FinnGen Ethics Statement

Patients and control subjects in FinnGen provided informed consent for biobank research, based on the Finnish Biobank Act. Alternatively, separate research cohorts, collected prior the Finnish Biobank Act came into effect (in September 2013) and start of FinnGen (August 2017), were collected based on study-specific consents and later transferred to the Finnish biobanks

after approval by Fimea (Finnish Medicines Agency), the National Supervisory Authority for Welfare and Health. Recruitment protocols followed the biobank protocols approved by Fimea. The Coordinating Ethics Committee of the Hospital District of Helsinki and Uusimaa (HUS) statement number for the FinnGen study is Nr HUS/990/2017.

The FinnGen study is approved by Finnish Institute for Health and Welfare (permit numbers: THL/2031/6.02.00/2017, THL/1101/5.05.00/2017, THL/341/6.02.00/2018, THL/2222/6.02.00/2018, THL/283/6.02.00/2019, THL/1721/5.05.00/2019 and THL/1524/5.05.00/2020), Digital and population data service agency (permit numbers: VRK43431/2017-3, VRK/6909/2018-3, VRK/4415/2019-3), the Social Insurance Institution (permit numbers: KELA 58/522/2017, KELA 131/522/2018, KELA 70/522/2019, KELA 98/522/2019, KELA 134/522/2019, KELA 138/522/2019, KELA 2/522/2020, KELA 16/522/2020), Findata permit numbers THL/2364/14.02/2020, THL/4055/14.06.00/2020, THL/3433/14.06.00/2020, THL/4432/14.06/2020, THL/5189/14.06/2020, THL/5894/14.06.00/2020, THL/6619/14.06.00/2020, THL/209/14.06.00/2021, THL/688/14.06.00/2021, THL/1284/14.06.00/2021, THL/1965/14.06.00/2021, THL/5546/14.02.00/2020, THL/2658/14.06.00/2021, THL/4235/14.06.00/2021, Statistics Finland (permit numbers: TK-53-1041-17 and TK/143/07.03.00/2020 (earlier TK-53-90-20) TK/1735/07.03.00/2021, TK/3112/07.03.00/2021) and Finnish Registry for Kidney Diseases permission/extract from the meeting minutes on 4th July 2019.

The Biobank Access Decisions for FinnGen samples and data utilized in FinnGen Data Freeze 10 include: THL Biobank BB2017_55, BB2017_111, BB2018_19, BB_2018_34, BB_2018_67, BB2018_71, BB2019_7, BB2019_8, BB2019_26, BB2020_1, BB2021_65, Finnish Red Cross Blood Service Biobank 7.12.2017, Helsinki Biobank HUS/359/2017, HUS/248/2020, HUS/150/2022 § 12, §13, §14, §15, §16, §17, §18, and §23, Auria Biobank AB17-5154 and

amendment #1 (August 17 2020) and amendments BB_2021-0140, BB_2021-0156 (August 26 2021, Feb 2 2022), BB_2021-0169, BB_2021-0179, BB_2021-0161, AB20-5926 and amendment #1 (April 23 2020)and it´s modification (Sep 22 2021), Biobank Borealis of Northern Finland_2017_1013, 2021_5010, 2021_5018, 2021_5015, 2021_5023, 2021_5017, 2022_6001, Biobank of Eastern Finland 1186/2018 and amendment 22 § /2020, 53§/2021, 13§/2022, 14§/2022, 15§/2022, Finnish Clinical Biobank Tampere MH0004 and amendments (21.02.2020 & 06.10.2020), §8/2021, §9/2022, §10/2022, §12/2022, §20/2022, §21/2022, §22/2022, §23/2022, Central Finland Biobank 1-2017, and Terveystalo Biobank STB 2018001 and amendment 25th Aug 2020, Finnish Hematological Registry and Clinical Biobank decision 18th June 2021, Arctic biobank P0844: ARC_2021_1001.

Endpoint definitions in FinnGen

We used the following FinnGen endpoints from Data Freeze 11: E4_DM2 (Type 2 diabetes), I9_AF (atrial fibrillation or flutter), I9_HEARTFAIL (heart failure), I9_CHD (Coronary artery disease), and I9_STR (stroke). FinnGen endpoint definitions incorporate International Classification of Diseases (ICD) codes from hospital, outpatient and cause-of-death registries; ICD or Social Insurance Institution (KELA) classification based medication reimbursement codes; and Anatomical Therapeutic Chemical codes for medication purchases. The definitions are publicly available at https://www.finngen.fi/en/researchers/clinical-endpoints and on https://risteys.finregistry.fi.

Gene prioritization

We used two approaches to prioritize potentially causative genes in the association loci: nearest protein-coding gene and Polygenic Priority Score (PoPS)[3]. To compute gene-specific PoPS, we first performed a gene-based analysis with MAGMA v1.10 using the default snp-wise=mean gene analysis model[4]. The raw gene-based results from MAGMA and the full set of default features provided by the PoPS authors were then used to calculate gene-specific PoPS. The

gene with the highest PoPS within +/- 500kb of the lead variant was designated as the gene prioritized by PoPS.

Genome-wide association study meta-analysis

We performed a p-value based sample size weighted meta-analysis of the UKB GWAS and a previously published GWAS meta-analysis (n = 12,204)[5,6] using METAL (version release 2020-05-05) without genomic control. We evaluated for the presence of inflation based on the LD score regression intercept for the novel meta-analysis.

Polygenic score analyses

We constructed a polygenic score (PGS) for PAT using the summary statistics from the UKB GWAS and the PRS-CS-auto tool with a UK Biobank European ancestry LD reference panel and HapMap3 variants[7]. We calculated individual-level PGSs using the resulting weights in FinnGen study participants with PLINK v2.0[8]. We evaluated the associations of the PAT PGS with cardiovascular diseases registered at any point before or after DNA sampling as outcomes, using logistic regression models with sex, age at the end of study follow-up or death, genomic principal components 1–5 and the genotyping array as basic covariates.

Supplementary Results

Genomic inflation and LD Score Regression Intercept

The genomic control inflation statistic (lambda) of the genome-wide association study of PAT in UKB was modestly elevated at 1.096 (Supplementary Figure 7), but the linkage disequilibrium score regression intercept was 1.00, consistent with true polygenic signal. Similarly, in the meta-analysis of the UKB GWAS and a previously published PAT GWAS meta-analysis[6], the genomic inflation factor was 1.103 and the LD score regression intercept was 1.0105 (SE 0.0075).

Supplementary Figures

Supplementary Figure 1: Study flowchart

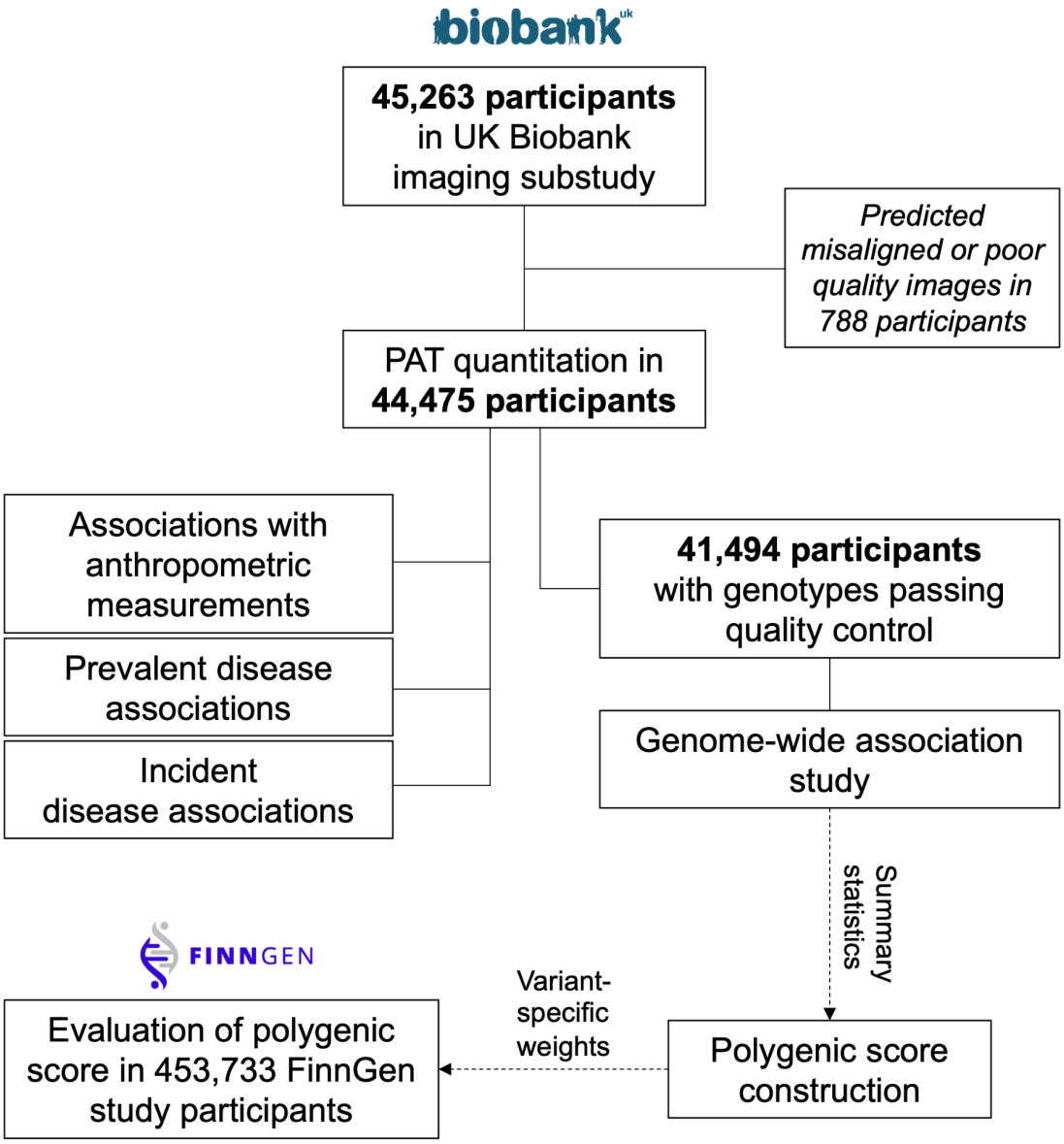

Supplementary Figure 2: The associations of pericardial adipose tissue with age, sex, and anthropometric measurements

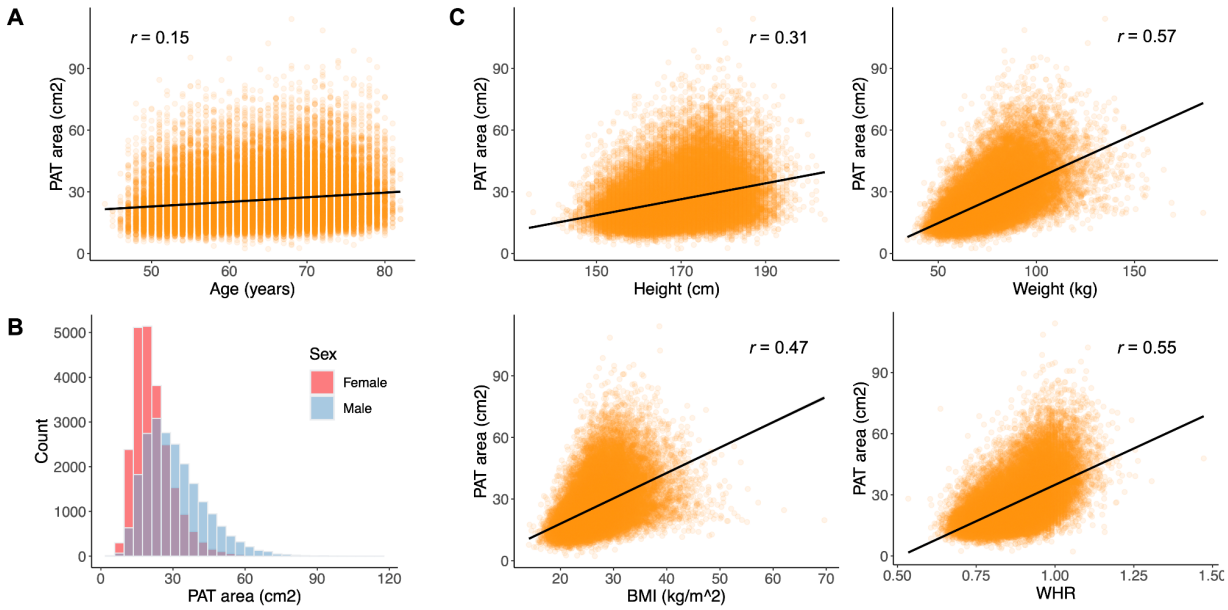

A. The association of PAT with age during the imaging visit. B. The distribution of PAT in women (red) and men (blue). C. The correlations of anthropometric measurements with pericardial adipose tissue. Pearson's correlation coefficient is shown for all pairs of continuous traits. Abbreviations: BMI = body mass index, PAT = pericardial adipose tissue, WHR = waist to hip ratio.

Supplementary Figure 3: The associations of pericardial adipose tissue with incident diseases

A. Adjusted for basic covariates

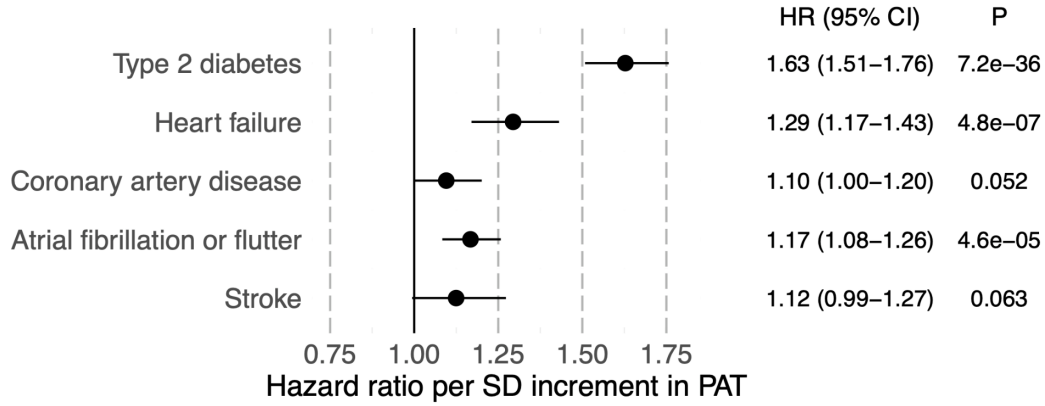

B. Adjusted for basic covariates and BMI

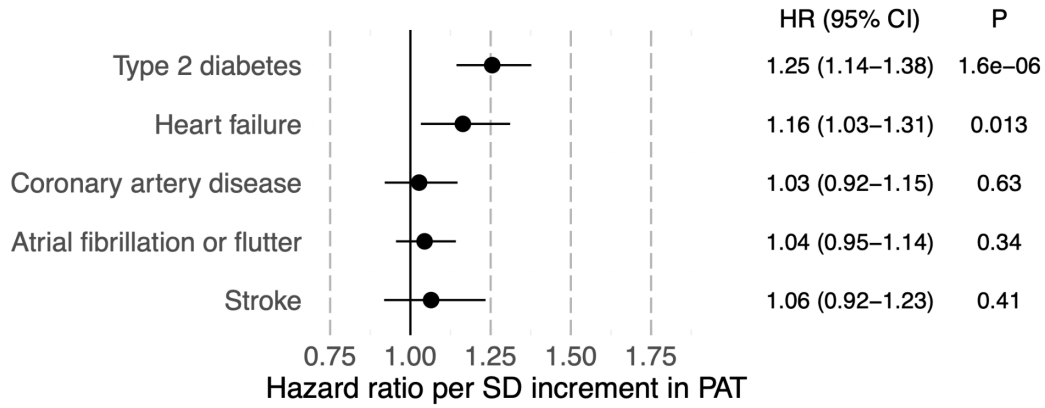

The associations of PAT with incident diseases were tested using Cox proportional hazards models with time from imaging to diagnosis or censoring as the outcome and PAT (standard deviation scaled), sex, and age as the predictors. Body mass index (BMI) was included as an additional covariate in BMI-adjusted models. Participants with the corresponding prevalent disease at the time of imaging were excluded from analyses. Effect estimates are reported for PAT. CI = confidence interval.

Supplementary Figure 4: The associations of percentile-stratified pericardial adipose tissue with incident diseases

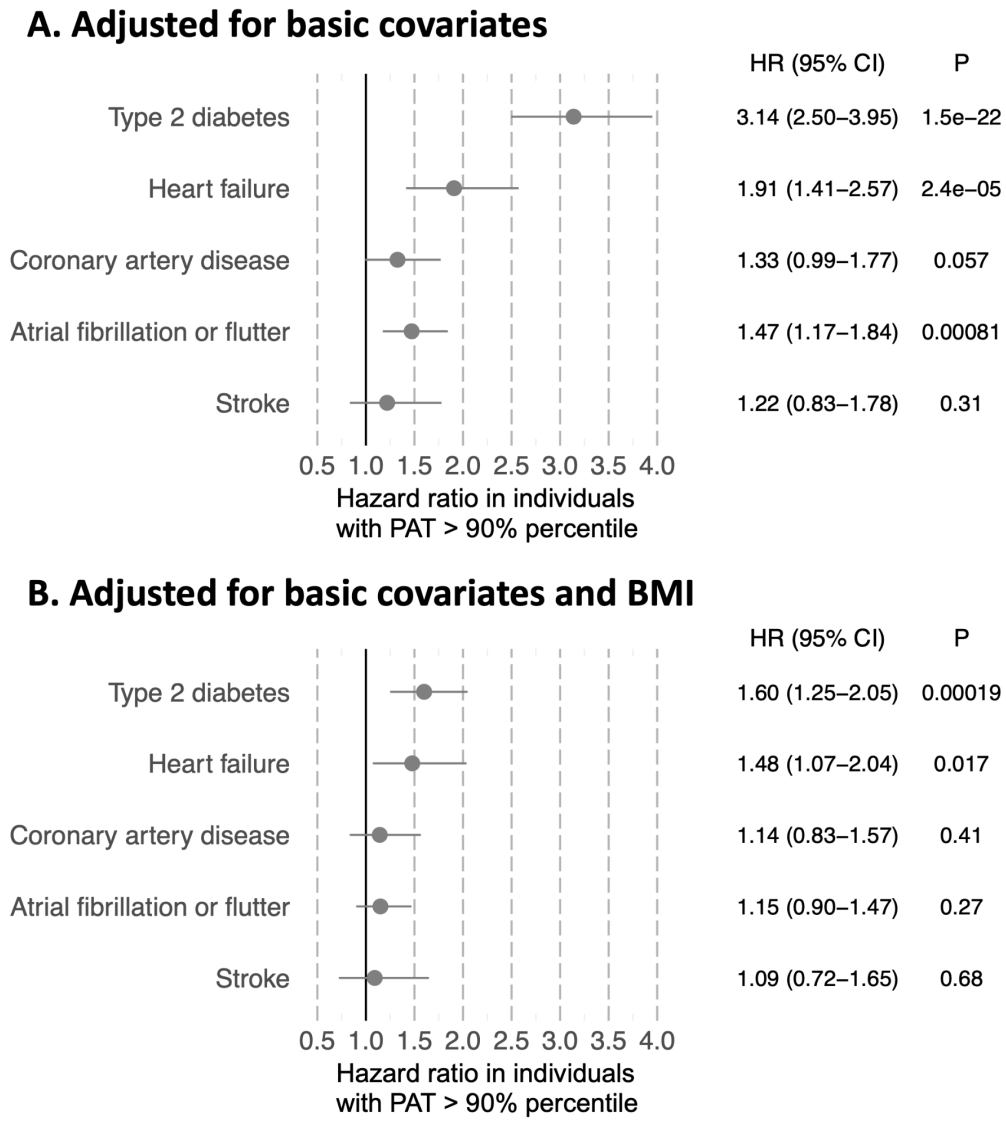

The associations of PAT with incident diseases were tested using Cox proportional hazards models with time from imaging to diagnosis or censoring as the outcome and PAT percentile (over 90th percentile vs. others), sex, and age as the predictors. Participants with the corresponding prevalent disease at the time of imaging were excluded from analyses. Body mass index (BMI) was included as an additional covariate in BMI-adjusted models. Hazard

ratios estimates are reported for the PAT strata (> 90th percentile compared with PAT ≤ 90th percentile)

Supplementary Figure 5: Cumulative incidences of cardiovascular diseases stratified by PAT decile at baseline

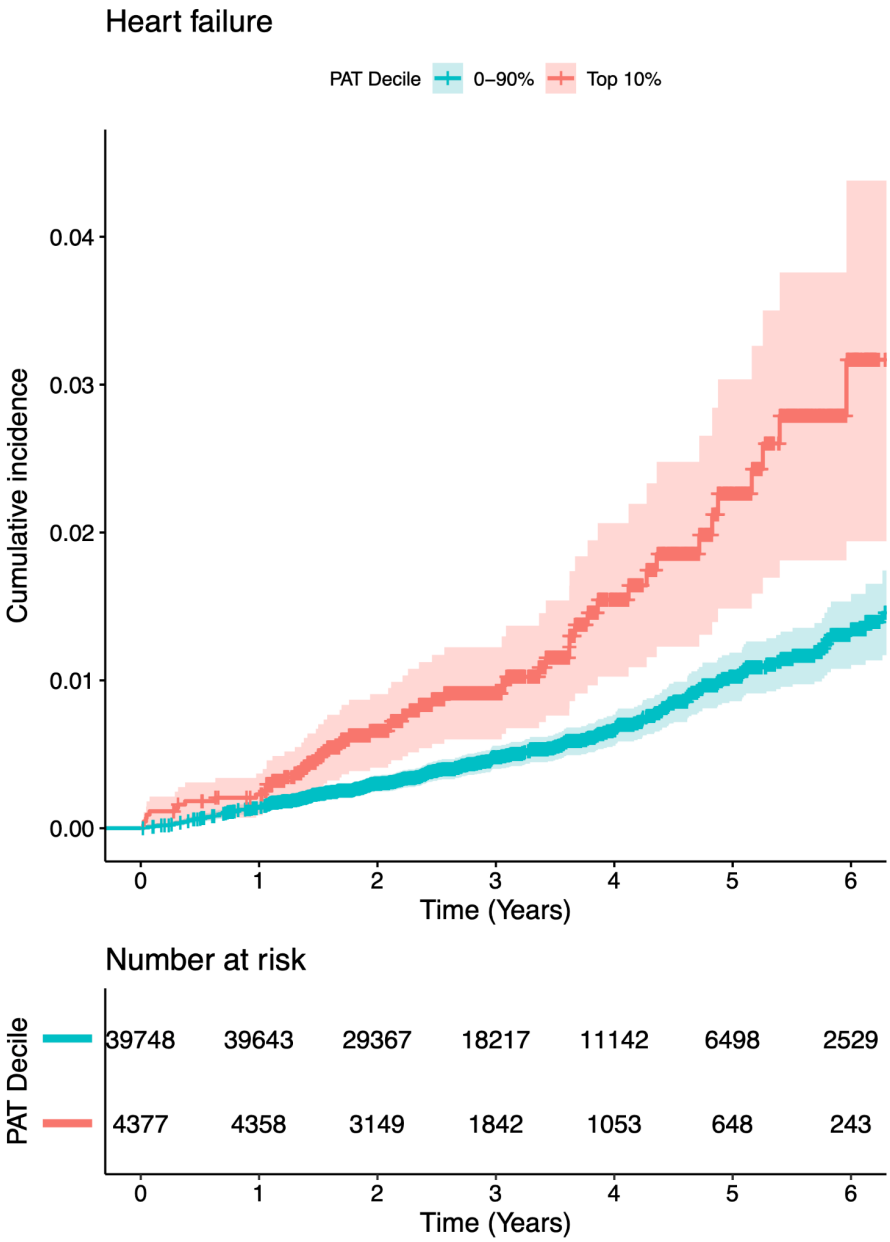

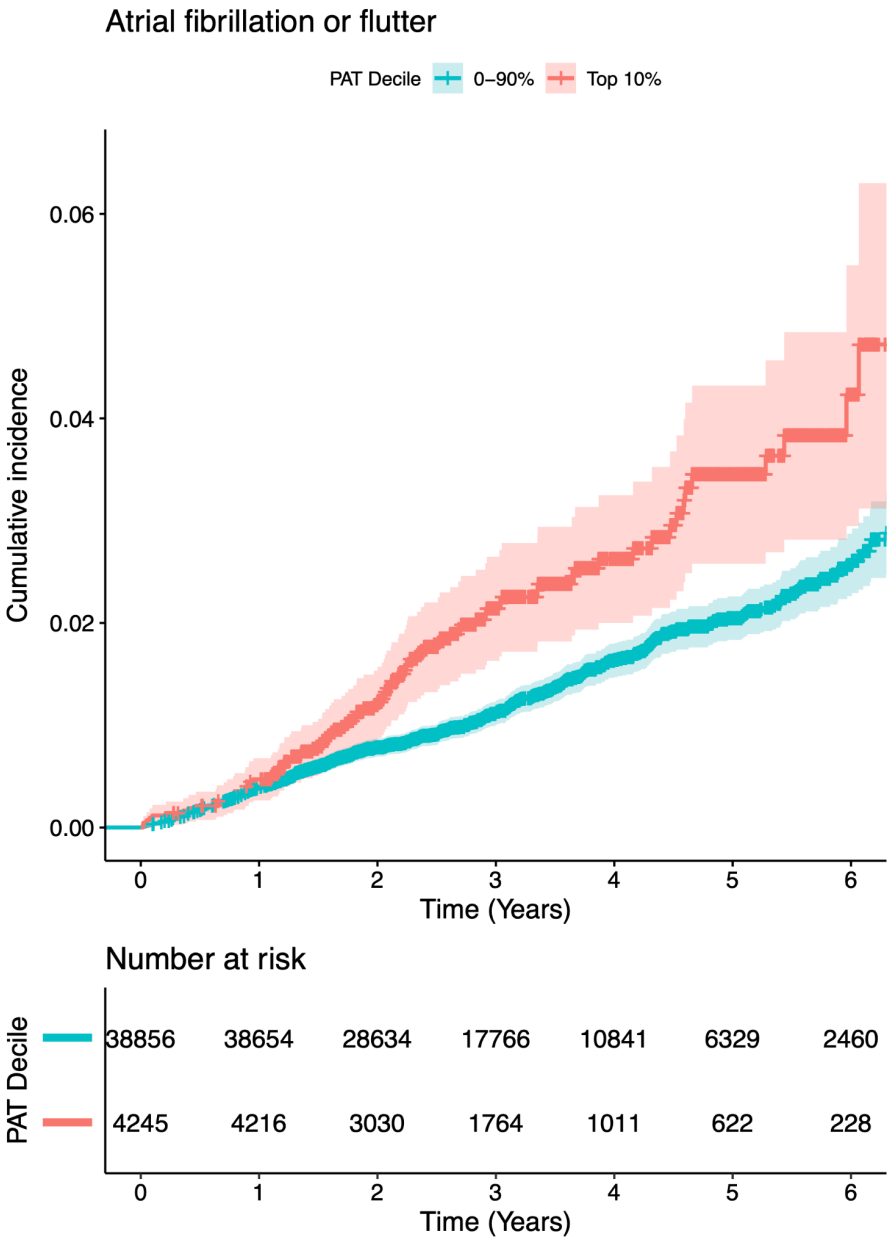
Atrial fibrillation or flutter
PAT Decile
0–90%
Top 10%
Cumulative incidence
0.06
0.04
0.02
0.00
0
1
2
3
4
5
6
Time (Years)
Number at risk
PAT Decile
38856
38654
28634
17766
10841
6329
2460
4245
4216
3030
1764
1011
622
228
0
1
2
3
4
5
6
Time (Years)

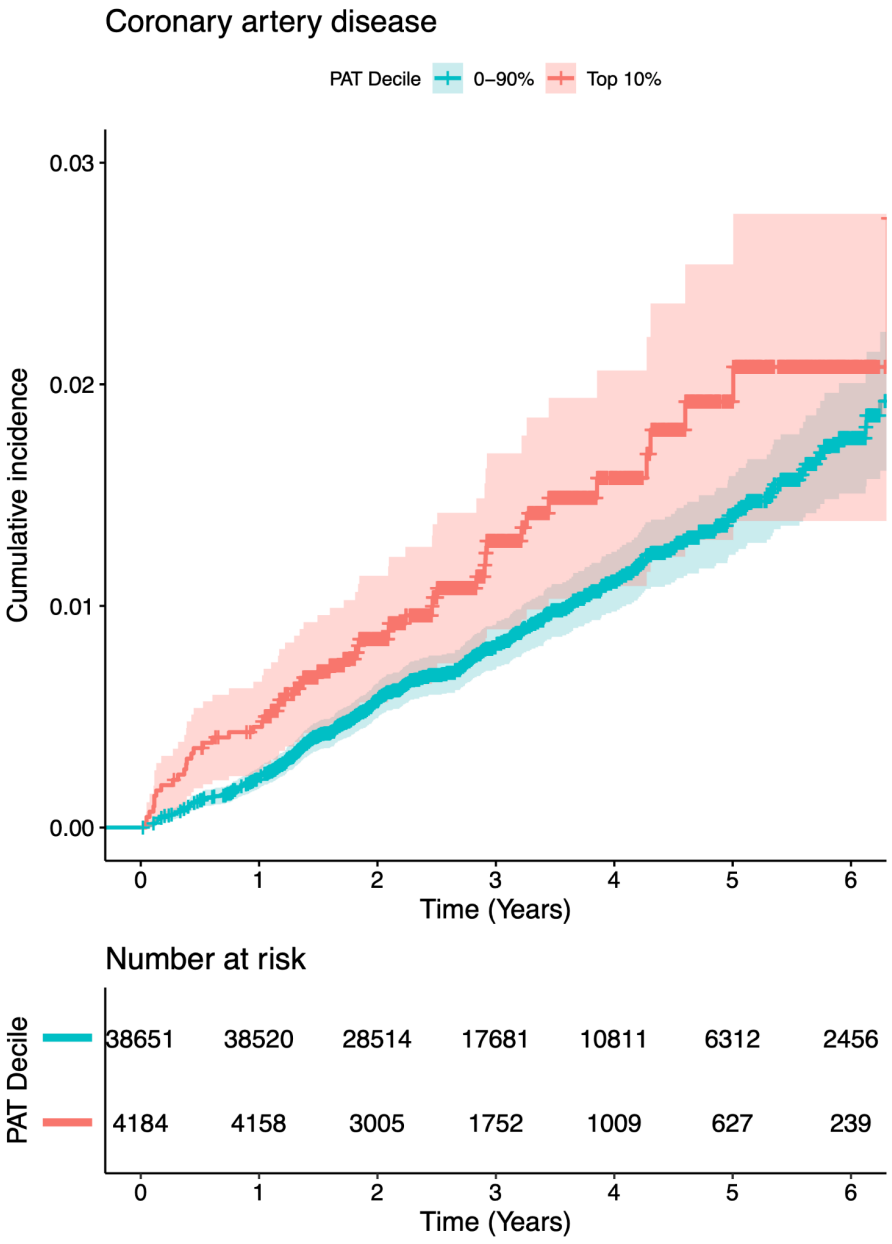
Coronary artery disease
PAT Decile
0–90%
Top 10%
0.03
0.02
0.01
0.00
Cumulative incidence
0
1
2
3
4
5
6
Time (Years)
Number at risk
PAT Decile
38651
38520
28514
17681
10811
6312
2456
4184
4158
3005
1752
1009
627
239
0
1
2
3
4
5
6
Time (Years)

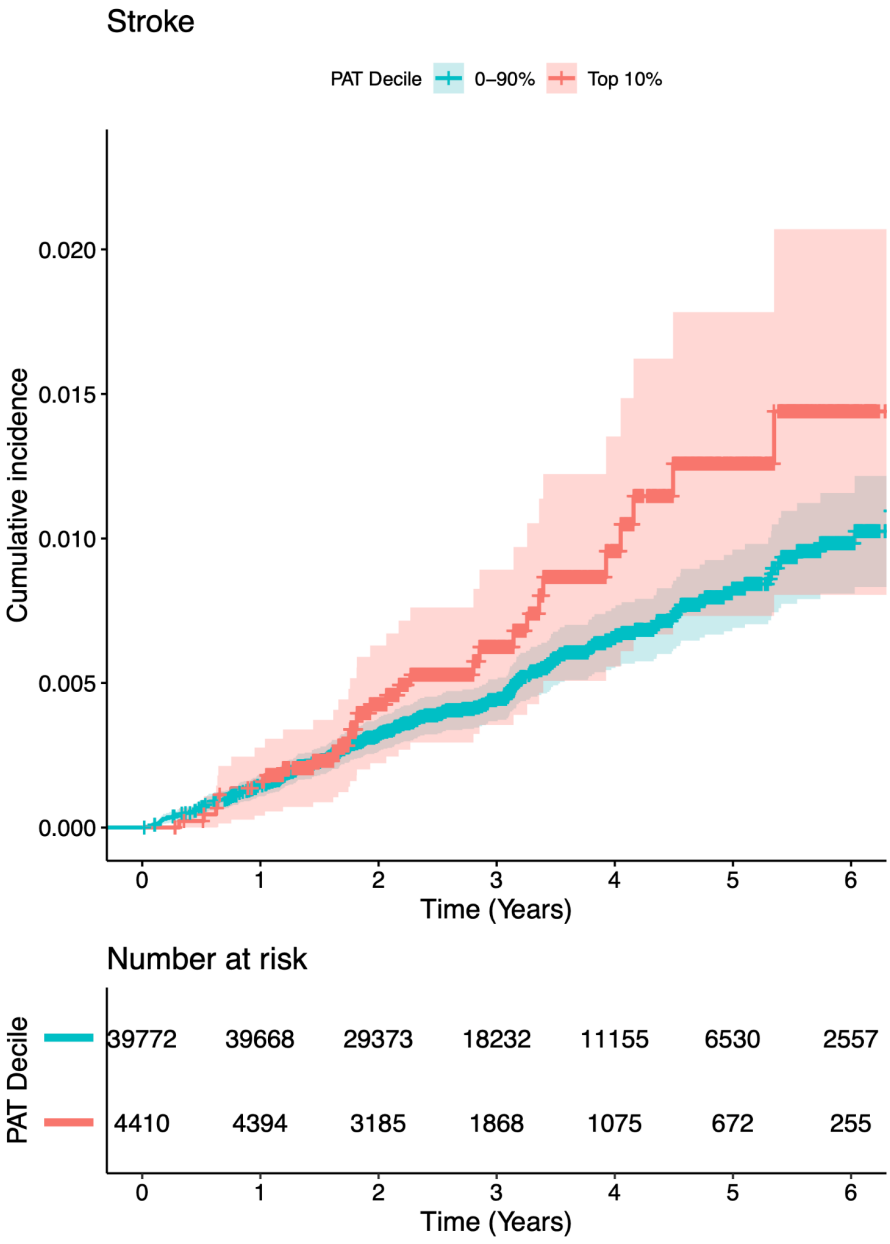
Stroke
PAT Decile
0–90%
Top 10%
Cumulative incidence
0.020
0.015
0.010
0.005
0.000
0
1
2
3
4
5
6
Time (Years)
Number at risk
PAT Decile
39772 39668 29373 18232 11155 6530 2557
4410 4394 3185 1868 1075 672 255
0
1
2
3
4
5
6
Time (Years)

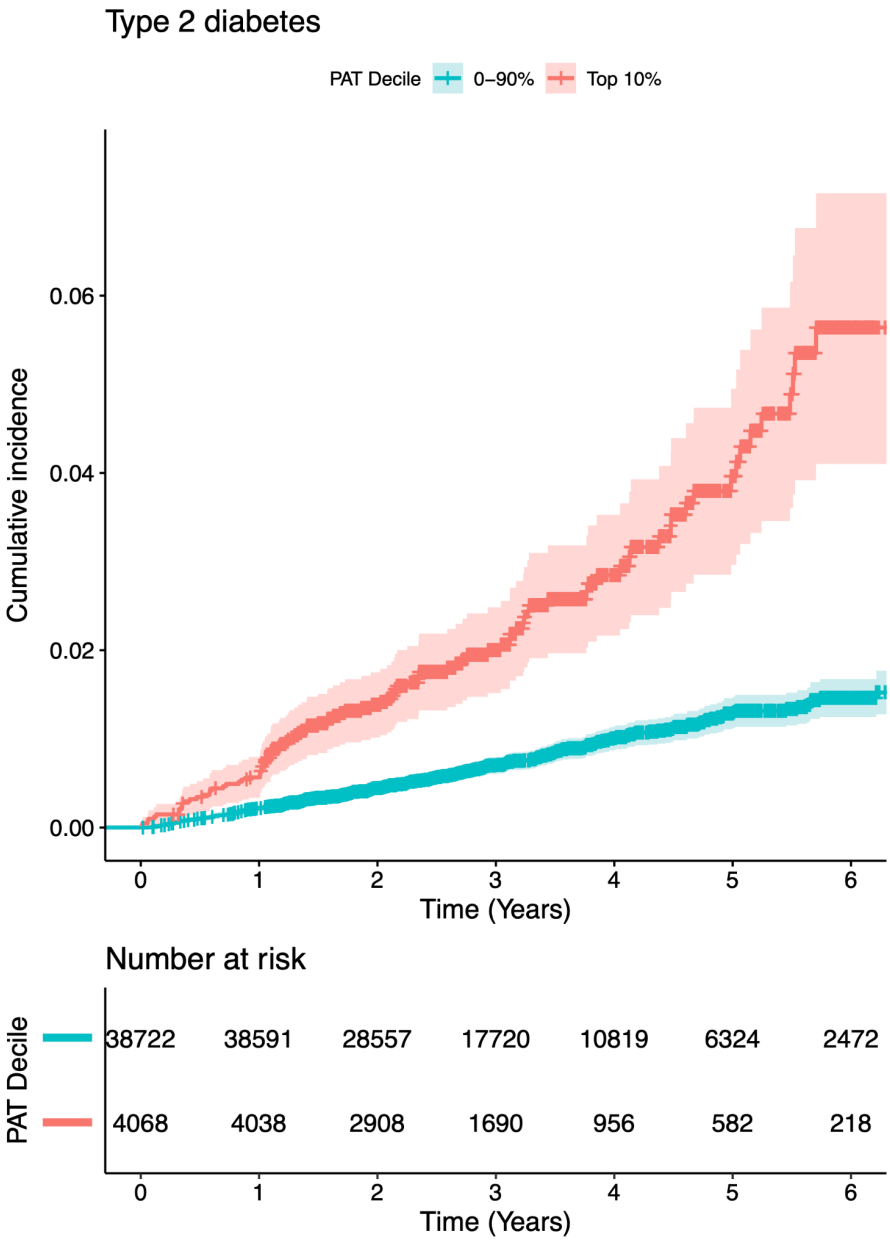
Type 2 diabetes
PAT Decile
0–90%
Top 10%
Cumulative incidence
0.06
0.04
0.02
0.00
0
1
2
3
4
5
6
Time (Years)
Number at risk
PAT Decile
38722
38591
28557
17720
10819
6324
2472
4068
4038
2908
1690
956
582
218
0
1
2
3
4
5
6
Time (Years)

Supplementary Figure 6: Locus plots from the genome-wide association study of pericardial adipose tissue in UK Biobank

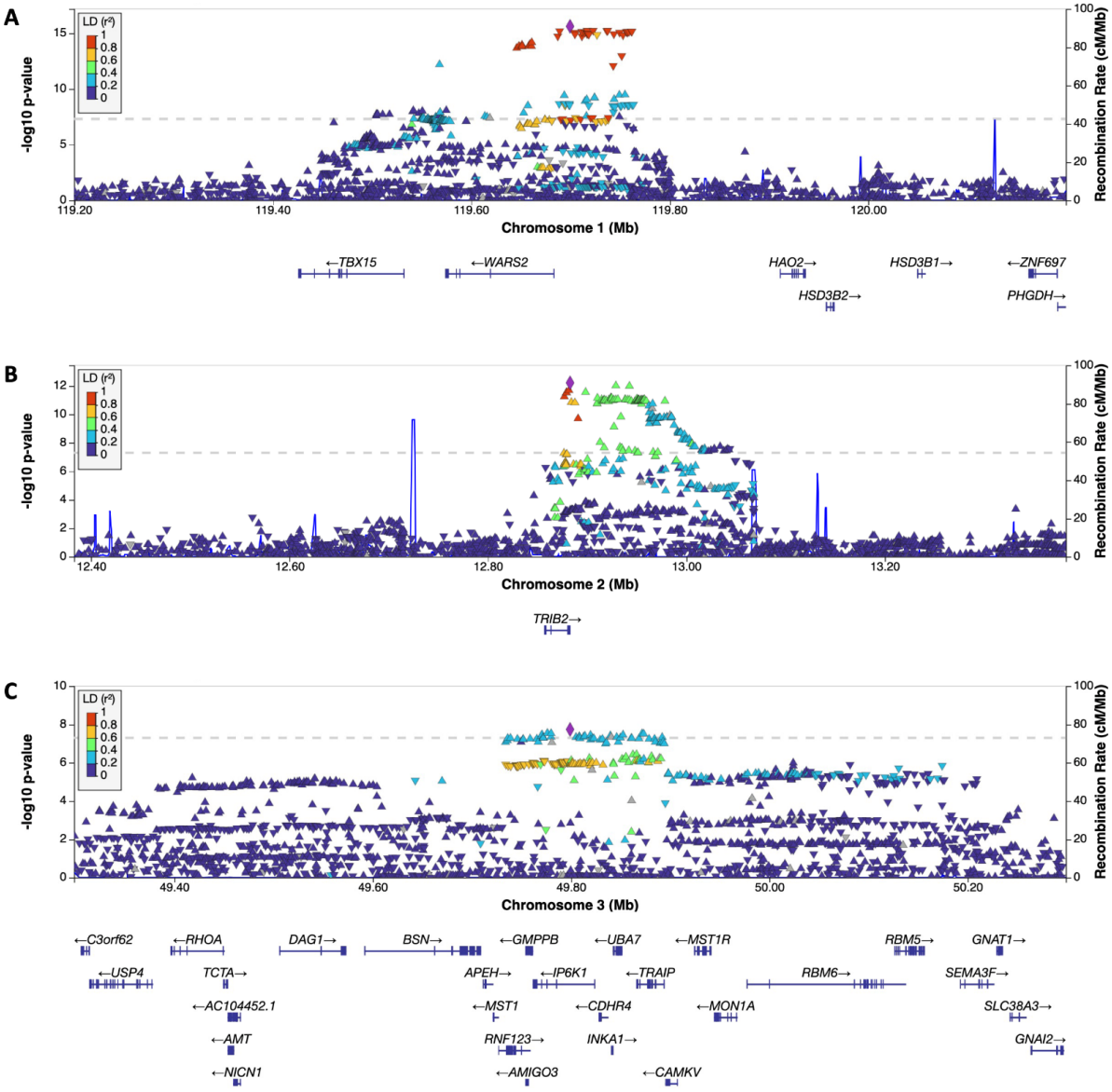

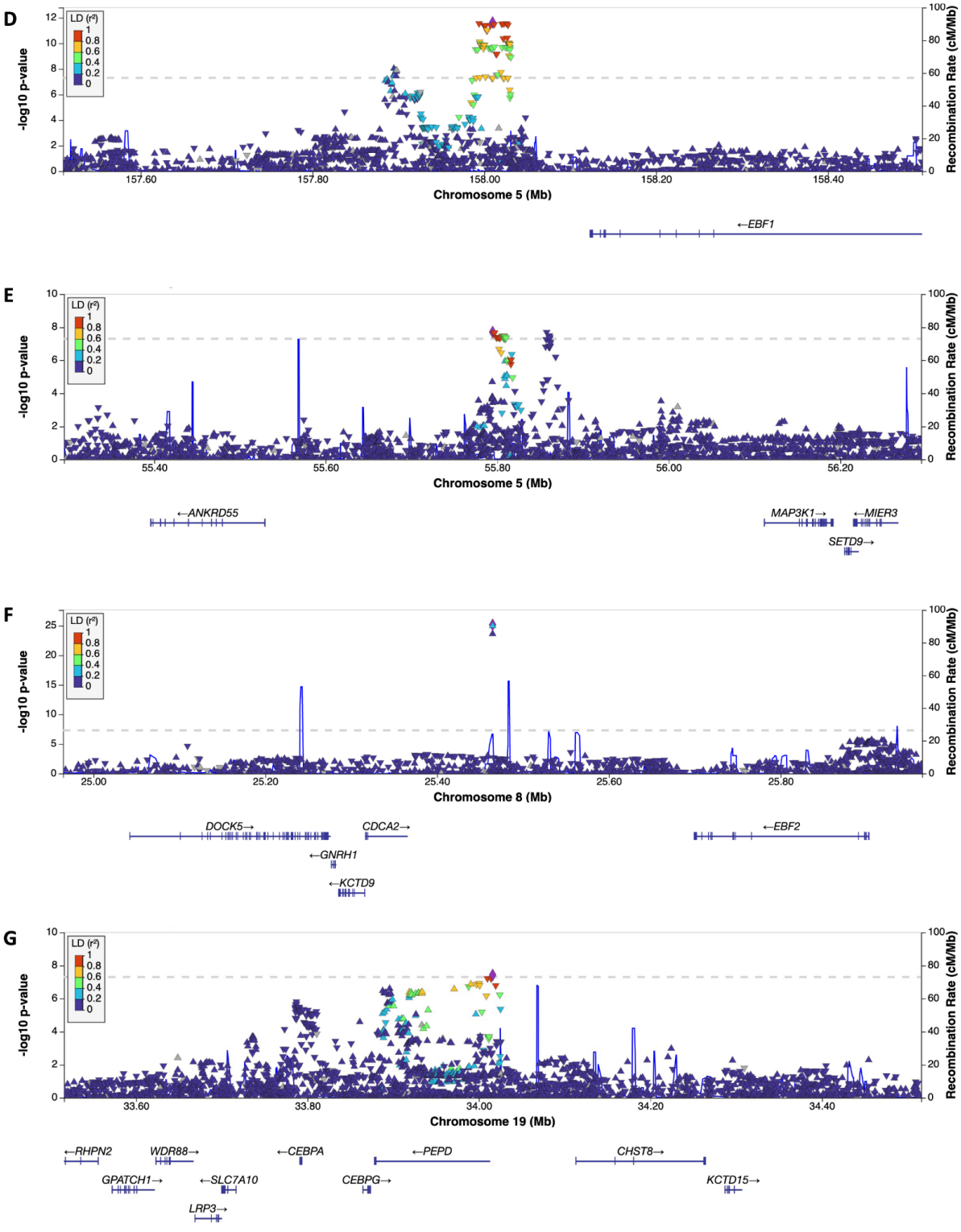
D
LD (r²)
1
0.8
0.6
0.4
0.2
0
-log10 p-value
Recombination Rate (cM/Mb)
157.60
157.80
158.00
158.20
158.40
Chromosome 5 (Mb)
←EBF1
E
55.40
55.60
55.80
56.00
56.20
Chromosome 5 (Mb)
←ANKRD55
MAP3K1→
←MIER3
SETD9→
F
25.00
25.20
25.40
25.60
25.80
Chromosome 8 (Mb)
DOCK5→
CDCA2→
←EBF2
←GNRH1
←KCTD9
G
33.60
33.80
34.00
34.20
34.40
Chromosome 19 (Mb)
←RHPN2
WDR88→
←CEBPA
←PEPD
CHST8→
GPATCH1→
←SLC7A10
CEBPG→
KCTD15→
LRP3→

Supplementary Figure 7: Quantile-quantile plot of p-values from the genome-wide association study of pericardial adipose tissue in UK Biobank

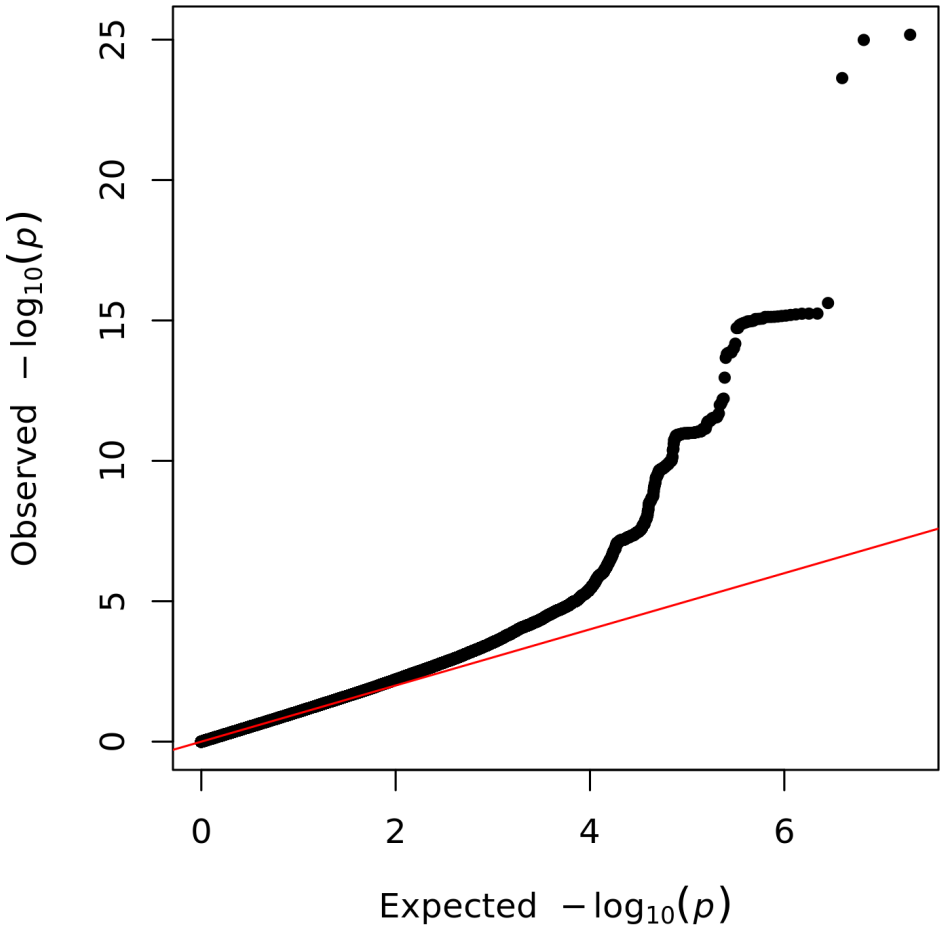

A genome-wide association study of pericardial adipose tissue was performed in 41,494 UK Biobank participants. Expected and observed p-values are shown on the -log10 scale.

Supplementary Figure 8: Manhattan plot of the meta-analysis of genome-wide association studies of pericardial adipose tissue

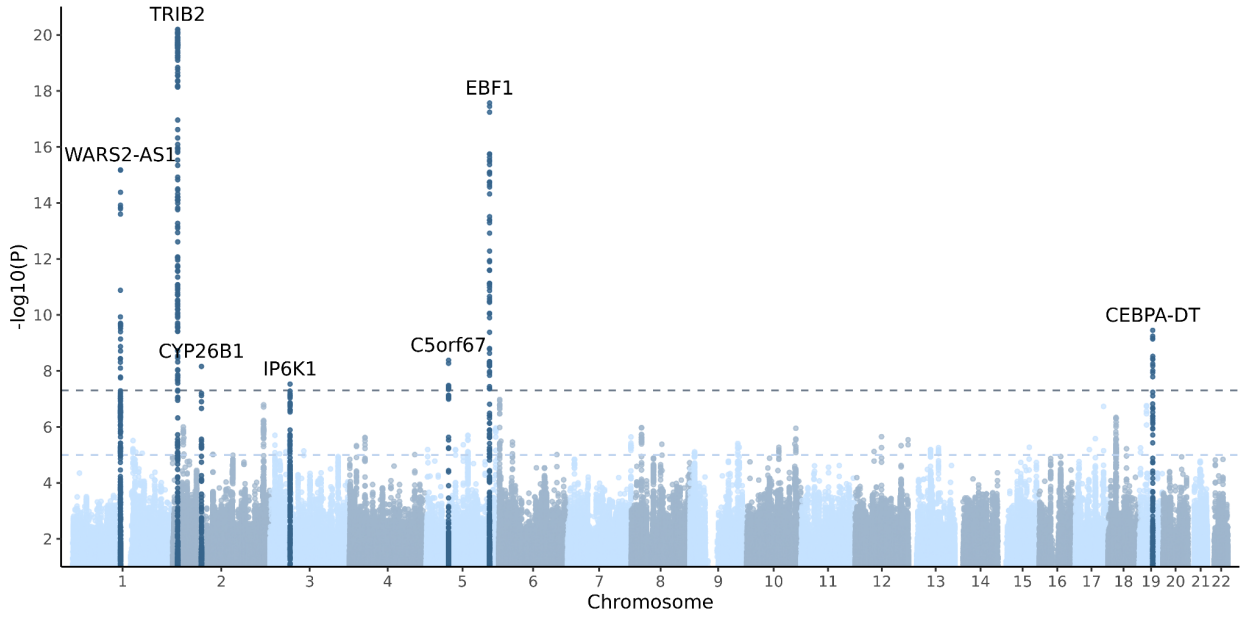

A p-value based sample size weighted meta-analysis of the UK Biobank genome-wide association study and a previously published GWAS meta-analysis by Chu et al (n = 12,204) was performed using METAL, including up to 53,698 total participants. Each variant is plotted as a data point, with the corresponding $-\log_{10}(P)$ shown on the y-axis and the genomic position shown on the x-axis grouped by chromosomes. The genome-wide significance threshold ($P = 5*10^{-8}$) is shown with a darker dashed line and a suggestive threshold ($P = 1*10^{-5}$) is shown with a lighter dashed line. Genomic loci with at least one variant reaching genome-wide significance are labeled with the name of the nearest gene, and all variants within 500 kilobases of the lead variant are coloured in a darker blue for visualization purposes. The y-axis is truncated to only show variants with a P-value ≤ 0.1.

Supplementary Figure 9: Quantile-quantile plot of the meta-analysis of genome-wide association studies of pericardial adipose tissue

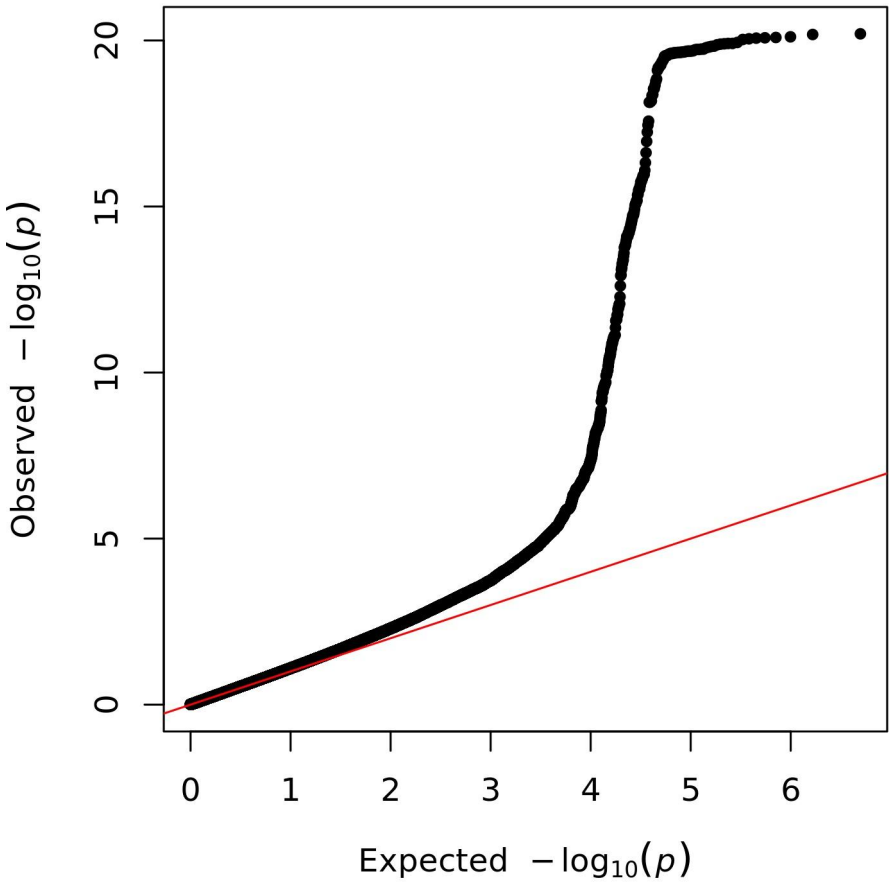

A p-value based sample size weighted meta-analysis of the UK Biobank genome-wide association study and a previously published GWAS meta-analysis by Chu et al (n = 12,204) was performed using METAL, including up to 53,698 total participants. Expected and observed p-values are shown on the -log10 scale.

Supplementary Tables

Supplementary Table 1: Characteristics of the study sample at the time of imaging and stratified by self-reported ethnic background

	White	Mixed ethnic background	Asian or Asian British	Black or Black British	Chinese	Other ethnic group
N	43014	204	482	301	129	226
Male sex (%)	20768 (48.3)	73 (35.8)	307 (63.7)	138 (45.8)	49 (38.0)	101 (44.7)
Age (mean (SD))	64.21 (7.71)	59.55 (7.75)	61.01 (8.44)	59.15 (7.26)	59.57 (6.80)	62.47 (8.04)
Height (mean (SD))	169.27 (9.24)	166.41 (8.69)	166.25 (8.81)	168.49 (9.51)	161.60 (7.60)	164.96 (9.80)
Weight (mean (SD))	76.15 (15.11)	75.17 (16.23)	72.00 (12.59)	82.07 (16.22)	62.26 (10.47)	73.65 (16.09)
Body mass index (mean (SD))	26.49 (4.37)	27.09 (5.24)	25.99 (3.73)	28.91 (5.30)	23.79 (3.17)	26.88 (4.42)
Waist circumference (mean (SD))	88.37 (12.73)	85.98 (12.75)	87.97 (10.76)	89.74 (12.60)	78.76 (9.70)	86.93 (13.30)
Hip circumference (mean (SD))	100.81 (8.70)	100.75 (10.64)	97.62 (7.90)	103.14 (10.26)	92.55 (6.66)	98.85 (9.48)
Waist-to-hip ratio (mean (SD))	0.88 (0.09)	0.85 (0.09)	0.90 (0.08)	0.87 (0.08)	0.85 (0.07)	0.88 (0.09)
PAT (mean (SD))	26.14 (11.45)	22.10 (10.02)	22.95 (9.26)	20.97 (7.92)	19.68 (8.05)	23.12 (10.29)
Diabetes type 2 (%)	1547 (3.6)	12 (5.9)	60 (12.4)	36 (12.0)	6 (4.7)	14 (6.2)
Heart failure (%)	304 (0.7)	2 (1.0)	5 (1.0)	1 (0.3)	0 (0.0)	3 (1.3)
Coronary artery disease (%)	1573 (3.7)	4 (2.0)	36 (7.5)	6 (2.0)	1 (0.8)	11 (4.9)
Atrial fibrillation or flutter (%)	1341 (3.1)	2 (1.0)	11 (2.3)	5 (1.7)	2 (1.6)	5 (2.2)
Stroke (%)	454 (1.1)	1 (0.5)	5 (1.0)	3 (1.0)	1 (0.8)	1 (0.4)

Baseline characteristics at the time of imaging are shown for UK Biobank cardiac magnetic resonance imaging substudy participants with automated pericardial adipose tissue (PAT) area quantitation from four-chamber images. Self-reported ancestry was used to stratify participants. Anthropometric measurements were taken during the imaging visit. Prevalent diseases were ascertained based on a combination of self-reported data and International Classification of Diseases codes.

Supplementary Table 2: UK Biobank Disease Definitions

Disease	Field ID	Description	Codes	Included / excluded
AF	20002	Non-cancer illness code, self-reported	14,711,483	Included
AF	20004	Operation code	1524	Included
AF	41202	Diagnoses - main ICD10	I48,I48.0,I48.1,I48.2,I48.3,I48.4,I48.9	Included
AF	41204	Diagnoses - secondary ICD10	I48,I48.0,I48.1,I48.2,I48.3,I48.4,I48.9	Included
AF	40001	Underlying (primary) cause of death: ICD10	I48,I48.0,I48.1,I48.2,I48.3,I48.4,I48.9	Included
AF	40002	Contributory (secondary) causes of death: ICD10	I48,I48.0,I48.1,I48.2,I48.3,I48.4,I48.9	Included
AF	41203	Diagnoses - main ICD9	4273	Included
AF	41205	Diagnoses - secondary ICD9	4273	Included
AF	41200	Operative procedures - main OPCS4	K57.1,K62.1,K62.2,K62.3,K62.4	Included
AF	41210	Operative procedures - secondary OPCS4	K57.1,K62.1,K62.2,K62.3,K62.4	Included
CAD	20002	Non-cancer illness code, self-reported	1075	Included
CAD	20004	Operation code	107,010,951,523	Included
CAD	6150	Vascular/heart problems diagnosed by doctor	1	Included
CAD	41202	Diagnoses - main ICD10	I21,I21.0,I21.1,I21.2,I21.3,I21.4,I21.9, I22,I22.0,I22.1	Included
CAD	41202	Diagnoses - main ICD10	I22.8,I22.9,I23,I23.0,I23.1,I23.2,I23.3, I23.4,I23.5,I23.6	Included
CAD	41202	Diagnoses - main ICD10	I23.8,I24,I24.0,I24.1,I24.8,I24.9,I25.2	Included
CAD	41204	Diagnoses - secondary ICD10	I21,I21.0,I21.1,I21.2,I21.3,I21.4,I21.9, I22,I22.0,I22.1	Included
CAD	41204	Diagnoses - secondary ICD10	I22.8,I22.9,I23,I23.0,I23.1,I23.2,I23.3, I23.4,I23.5,I23.6	Included
CAD	41204	Diagnoses - secondary ICD10	I23.8,I24,I24.0,I24.1,I24.8,I24.9,I25.2	Included
CAD	40001	Underlying (primary) cause of death: ICD10	I21,I21.0,I21.1,I21.2,I21.3,I21.4,I21.9, I22,I22.0,I22.1	Included
CAD	40001	Underlying (primary) cause of death: ICD10	I22.8,I22.9,I23,I23.0,I23.1,I23.2,I23.3, I23.4,I23.5,I23.6	Included

CAD	40001	Underlying (primary) cause of death: ICD10	I23.8,I24,I24.0,I24.1,I24.8,I24.9,I25.2	Included
CAD	40002	Contributory (secondary) causes of death: ICD10	I21,I21.0,I21.1,I21.2,I21.3,I21.4,I21.9,I22,I22.0,I22.1	Included
CAD	40002	Contributory (secondary) causes of death: ICD10	I22.8,I22.9,I23,I23.0,I23.1,I23.2,I23.3,I23.4,I23.5,I23.6	Included
CAD	40002	Contributory (secondary) causes of death: ICD10	I23.8,I24,I24.0,I24.1,I24.8,I24.9,I25.2	Included
CAD	41200	Operative procedures - main OPCS4	K40,K40.1,K40.2,K40.3,K40.4,K40.8,K40.9,K41,K41.1,K41.2	Included
CAD	41200	Operative procedures - main OPCS4	K41.3,K41.4,K41.8,K41.9,K42,K42.1,K42.2,K42.3,K42.4,K42.8	Included
CAD	41200	Operative procedures - main OPCS4	K42.9,K43,K43.1,K43.2,K43.3,K43.4,K43.8,K43.9,K44,K44.1	Included
CAD	41200	Operative procedures - main OPCS4	K44.2,K44.8,K44.9,K45.1,K45.2,K45.3,K45.4,K45.5,K45.6,K45.8	Included
CAD	41200	Operative procedures - main OPCS4	K45.9,K46,K46.1,K46.2,K46.3,K46.4,K46.5,K46.8,K46.9,K49.1	Included
CAD	41200	Operative procedures - main OPCS4	K49.2,K49.3,K49.4,K49.8,K49.9,K50.1,K50.2,K50.4,K75.1,K75.2	Included
CAD	41200	Operative procedures - main OPCS4	K75.3,K75.4,K75.8,K75.9	Included
CAD	41210	Operative procedures - secondary OPCS4	K40,K40.1,K40.2,K40.3,K40.4,K40.8,K40.9,K41,K41.1,K41.2	Included
CAD	41210	Operative procedures - secondary OPCS4	K41.3,K41.4,K41.8,K41.9,K42,K42.1,K42.2,K42.3,K42.4,K42.8	Included
CAD	41210	Operative procedures - secondary OPCS4	K42.9,K43,K43.1,K43.2,K43.3,K43.4,K43.8,K43.9,K44,K44.1	Included
CAD	41210	Operative procedures - secondary OPCS4	K44.2,K44.8,K44.9,K45.1,K45.2,K45.3,K45.4,K45.5,K45.6,K45.8	Included
CAD	41210	Operative procedures - secondary OPCS4	K45.9,K46,K46.1,K46.2,K46.3,K46.4,K46.5,K46.8,K46.9,K49.1	Included
CAD	41210	Operative procedures - secondary OPCS4	K49.2,K49.3,K49.4,K49.8,K49.9,K50.1,K50.2,K50.4,K75.1,K75.2	Included
CAD	41210	Operative procedures - secondary OPCS4	K75.3,K75.4,K75.8,K75.9	Included
CAD	41203	Diagnoses - main ICD9	410,410,941,141,194,000,000	Included
CAD	41205	Diagnoses - secondary ICD9	410,410,941,141,194,000,000	Included

T2D	20002	Non-cancer illness code, self-reported	1223	Included
T2D	41202	Diagnoses - main ICD10	E11,E11.0,E11.1,E11.2,E11.3,E11.4,E11.5,E11.6,E11.7,E11.8,E11.9	Included
T2D	41204	Diagnoses - secondary ICD10	E11,E11.0,E11.1,E11.2,E11.3,E11.4,E11.5,E11.6,E11.7,E11.8,E11.9	Included
T2D	40001	Underlying (primary) cause of death: ICD10	E11,E11.0,E11.1,E11.2,E11.3,E11.4,E11.5,E11.6,E11.7,E11.8,E11.9	Included
T2D	40002	Contributory (secondary) causes of death: ICD10	E11,E11.0,E11.1,E11.2,E11.3,E11.4,E11.5,E11.6,E11.7,E11.8,E11.9	Included
HF	20002	Non-cancer illness code, self-reported	10,761,079	Included
HF	41202	Diagnoses - main ICD10	I11.0,I13.0,I13.2,I25.5,I42.0,I42.5,I42.8,I42.9,I50,I50.0,I50.1,I50.9	Included
HF	41204	Diagnoses - secondary ICD10	I11.0,I13.0,I13.2,I25.5,I42.0,I42.5,I42.8,I42.9,I50,I50.0,I50.1,I50.9	Included
HF	40001	Underlying (primary) cause of death: ICD10	I11.0,I13.0,I13.2,I25.5,I42.0,I42.5,I42.8,I42.9,I50,I50.0,I50.1,I50.9,4289	Included
HF	40002	Contributory (secondary) causes of death: ICD10	I11.0,I13.0,I13.2,I25.5,I42.0,I42.5,I42.8,I42.9,I50,I50.0,I50.1,I50.9,4289	Included
HF	41203	Diagnoses - main ICD9	425,442,804,281	Included
HF	41205	Diagnoses - secondary ICD9	425,442,804,281	Included
HF	20002	Non-cancer illness code, self-reported	1588	Excluded
HF	41202	Diagnoses - main ICD10	I42.1,I42.2	Excluded
HF	41204	Diagnoses - secondary ICD10	I42.1,I42.2	Excluded
HF	40001	Underlying (primary) cause of death: ICD10	I42.1,I42.2	Excluded
HF	40002	Contributory (secondary) causes of death: ICD10	I42.1,I42.2	Excluded
Stroke	42007	Source of stroke report	0,1,2	Included

Cardiovascular diseases in UK Biobank were defined using a combination of International Classification of Diseases (ICD) codes, self-report, and procedure codes. AF = atrial fibrillation or flutter, CAD = coronary artery disease, HF = heart failure, T2D = type 2 diabetes.

Supplementary Table 3: Prevalent disease association results in the UK Biobank

Disease	Cases	Controls	Beta	SE	Z	P
Type 2 diabetes	1679	42796	0.55795023	0.02266754	24.6144985	6.88E-133
Coronary artery disease	1634	42841	0.22275325	0.0233208	9.55170028	1.34E-21
Heart failure	316	44153	0.458047	0.05158378	8.87967091	6.95E-19
Atrial fibrillation or flutter	1368	43107	0.17963635	0.02526582	7.10985515	1.18E-12
Stroke	287	44188	0.09363106	0.05410968	1.73039391	0.08356686

In linear regression models, standard deviation scaled pericardial adipose tissue was used as the outcome and prevalent disease status (at the time of imaging), age and sex were used as the predictors. The effect (beta) estimates correspond to the differences in pericardial adipose tissue (in SD units) between individuals with prevalent disease and without prevalent disease.

Supplementary Table 4: The associations of pericardial adipose tissue with incident diseases

Model	Outcome	Cases	Controls	Z	P	HR	HR lower 95% CI	HR upper 95% CI
Basic	Type 2 diabetes	394	42402	12.50	7.22E-36	1.63	1.51	1.76
Basic	Heart failure	281	43872	5.03	4.83E-07	1.29	1.17	1.43
Basic	Atrial fibrillation or flutter	594	42513	4.07	4.64E-05	1.17	1.08	1.26
Basic	Coronary artery disease	403	42438	1.94	0.05228927	1.10	1.00	1.20
Basic	Stroke	238	43950	1.86	0.06274115	1.12	0.99	1.27
BMI-adjusted	Type 2 diabetes	394	42402	4.79	1.63E-06	1.25	1.14	1.38
BMI-adjusted	Heart failure	281	43872	2.49	0.01287948	1.16	1.03	1.31
BMI-adjusted	Atrial fibrillation or flutter	594	42513	0.95	0.34191072	1.04	0.96	1.14
BMI-adjusted	Stroke	238	43950	0.83	0.40801076	1.06	0.92	1.23
BMI-adjusted	Coronary artery disease	403	42438	0.48	0.63283322	1.03	0.92	1.15

The associations of PAT with incident diseases were tested using Cox proportional hazards models with time from imaging to diagnosis or censoring as the outcome and PAT (standard deviation scaled), sex, and age as the predictors. Body mass index (BMI) was included as an additional covariate in BMI-adjusted models. Participants with the corresponding prevalent disease at the time of imaging were excluded from analyses. Effect estimates are reported for PAT. CI = confidence interval, HR = hazard ratio.

Supplementary Table 5: The associations of percentile-stratified pericardial adipose tissue with incident diseases

Model	Outcome	Cases	Controls	Z	P	HR	HR lower 95% CI	HR upper 95% CI
Basic	Type 2 diabetes	394	42402	9.77	1.50E-22	3.14	2.50	3.95
Basic	Heart failure	281	43872	4.22	2.39E-05	1.91	1.41	2.57
Basic	Atrial fibrillation or flutter	594	42513	3.35	0.00080946	1.47	1.17	1.84
Basic	Coronary artery disease	403	42438	1.91	0.05662123	1.33	0.99	1.77
Basic	Stroke	238	43950	1.02	3.06E-01	1.22	0.83	1.78
BMI-adjusted	Type 2 diabetes	394	42402	3.73	0.00019376	1.60	1.25	2.05
BMI-adjusted	Heart failure	281	43872	2.38	0.01741983	1.48	1.07	2.04
BMI-adjusted	Atrial fibrillation or flutter	594	42513	1.11	0.26531812	1.15	0.90	1.47
BMI-adjusted	Coronary artery disease	403	42438	0.83	0.40808567	1.14	0.83	1.57
BMI-adjusted	Stroke	238	43950	0.41	0.68065094	1.09	0.72	1.65

The associations of PAT with incident diseases were tested using Cox proportional hazards models with time from imaging to diagnosis or censoring as the outcome and PAT percentile (over 90th percentile vs. others), sex, and age as the predictors. Participants with the corresponding prevalent disease at the time of imaging were excluded from analyses. Body mass index (BMI) was included as an additional covariate in BMI-adjusted models. Effect estimates are reported for the PAT strata (> 90th percentile compared with PAT ≤ 90th percentile). CI = confidence interval, HR = hazard ratio.

Supplementary Table 6: Polygenic priority scores for genes in genome-wide significant loci in the genome-wide association study of pericardial adipose tissue in UK Biobank

Locus	Min pos	Max pos	ENSGID	Name	PoPS	Start	End	TSS
1	119199426	120199426	ENSG00000116874	WARS2	1.03888821	119573839	119683294	119683294
1	119199426	120199426	ENSG00000092607	TBX15	0.97657313	119425669	119532179	119532179
1	119199426	120199426	ENSG00000203857	HSD3B1	0.23222331	120049821	120057681	120049821
1	119199426	120199426	ENSG00000143067	ZNF697	0.05501743	120162045	120190396	120190396
1	119199426	120199426	ENSG00000203859	HSD3B2	-0.0329964	119957554	119965658	119957554
1	119199426	120199426	ENSG00000116882	HAO2	-0.2148152	119911402	119936753	119911402
2	12382822	13382822	ENSG00000071575	TRIB2	1.58198676	12857015	12882860	12857015
3	49299046	50299046	ENSG00000004534	RBM6	0.60043145	49977440	50137478	49977440
3	49299046	50299046	ENSG00000233276	GPX1	0.52725384	49394609	49396033	49396033
3	49299046	50299046	ENSG00000173402	DAG1	0.49902449	49506146	49573048	49506146
3	49299046	50299046	ENSG00000001617	SEMA3F	0.49041147	50192478	50226508	50192478
3	49299046	50299046	ENSG00000067560	RHOA	0.4330987	49396578	49450431	49450431
3	49299046	50299046	ENSG00000164068	RNF123	0.42887217	49726932	49758962	49726932
3	49299046	50299046	ENSG00000176095	IP6K1	0.36463148	49761727	49823975	49823975
3	49299046	50299046	ENSG00000003756	RBM5	0.32854133	50126341	50156454	50126341
3	49299046	50299046	ENSG00000145020	AMT	0.22330205	49454211	49460186	49460186
3	49299046	50299046	ENSG00000188315	C3orf62	0.21420054	49306035	49315342	49315342
3	49299046	50299046	ENSG00000164078	MST1R	0.17829801	49924435	49941299	49941299
3	49299046	50299046	ENSG00000145022	TCTA	0.17811643	49449639	49453908	49449639

3	49299046	50299046	ENSG00000164077	MON1A	0.17742103	49946302	49967606	49967606
3	49299046	50299046	ENSG00000164062	APEH	0.16471345	49711435	49721396	49711435
3	49299046	50299046	ENSG00000164076	CAMKV	0.12723149	49895421	49907655	49907655
3	49299046	50299046	ENSG00000182179	UBA7	0.12413841	49842640	49851379	49851379
3	49299046	50299046	ENSG00000114316	USP4	0.11628078	49315264	49378145	49378145
3	49299046	50299046	ENSG00000173531	MST1	0.08499937	49721380	49726934	49726934
3	49299046	50299046	ENSG00000164061	BSN	0.0497476	49591922	49708978	49591922
3	49299046	50299046	ENSG00000187492	CDHR4	0.04815737	49828165	49837268	49837268
3	49299046	50299046	ENSG00000185614	FAM212A	0.0455302	49840687	49842463	49840687
3	49299046	50299046	ENSG00000173540	GMPPB	0.03592265	49754277	49761384	49761384
3	49299046	50299046	ENSG00000176020	AMIGO3	-0.0764481	49754267	49761349	49761349
3	49299046	50299046	ENSG00000114353	GNAI2	-0.0862229	50263724	50296787	50263724
3	49299046	50299046	ENSG00000145029	NICN1	-0.1067876	49460379	49466759	49466759
3	49299046	50299046	ENSG00000183763	TRAIP	-0.1813272	49866034	49894007	49894007
3	49299046	50299046	ENSG00000114349	GNAT1	-0.3860586	50229045	50233949	50229045
4	157509651	158509651	ENSG00000164330	EBF1	0.61142758	158122928	158526769	158526769
5	55294632	56294632	ENSG00000155545	MIER3	0.47698095	56215429	56267502	56267502
5	55294632	56294632	ENSG00000155542	SETD9	0.07370149	56205087	56221359	56205087
5	55294632	56294632	ENSG00000095015	MAP3K1	-0.1125205	56111401	56191979	56111401
5	55294632	56294632	ENSG00000164512	ANKRD55	-0.2717545	55395507	55529186	55529186
6	24964670	25964670	ENSG00000221818	EBF2	1.86841812	25699246	25902913	25902913
6	24964670	25964670	ENSG00000147459	DOCK5	1.01477449	25042238	25275598	25042238
6	24964670	25964670	ENSG00000104756	KCTD9	0.36411649	25285366	25315992	25315992
6	24964670	25964670	ENSG00000147437	GNRH1	0.24394595	25276776	25282170	25282170

6	24964670	25964670	ENSG00000184661	CDCA2	-0.2873648	25316513	25365436	25316513
7	33515904	34515904	ENSG00000245848	CEBPA	2.19365014	33790840	33793470	33793470
7	33515904	34515904	ENSG00000124299	PEPD	0.73815334	33877856	34012700	34012700
7	33515904	34515904	ENSG00000153885	KCTD15	0.37410233	34286838	34306668	34286838
7	33515904	34515904	ENSG00000153879	CEBPG	0.2954409	33864236	33873592	33864236
7	33515904	34515904	ENSG00000076650	GPATCH1	0.17831111	33571786	33621448	33571786
7	33515904	34515904	ENSG00000131941	RHPN2	0.14773468	33469499	33555794	33555794
7	33515904	34515904	ENSG00000130881	LRP3	0.03669161	33668509	33698694	33668509
7	33515904	34515904	ENSG00000166359	WDR88	-0.0535222	33622996	33666701	33622996
7	33515904	34515904	ENSG00000130876	SLC7A10	-0.1138438	33699570	33716756	33716756
7	33515904	34515904	ENSG00000124302	CHST8	-0.2077671	34112861	34264414	34112861

Polygenic Priority Scores (PoPS) were calculated for all genes within +/- 500,000kb of the lead variant in each genome-wide significant locus. “Min pos” and “Max pos” correspond to the locus boundaries. Start and End correspond to the regions of each gene. TSS = Transcription Start Site.

Supplementary Table 7: Genetic correlations between pericardial adipose tissue and anthropometric traits

Phenotype 1	Phenotype 2	rg	se	z	p
PAT	Height	0.05	0.05	1.00	0.32
PAT	Weight	0.48	0.04	11.37	5.93E-30
PAT	BMI	0.50	0.04	11.40	4.29E-30
PAT	WHR	0.60	0.05	11.44	2.69E-30

Genetic correlations between pericardial adipose tissue (PAT) and anthropometric measurements were calculated based on the summary statistics from genome-wide association studies in the UKB imaging substudy, using LD Score Regression with HapMap3 variants and a European ancestry reference panel. rg = genetic correlation, se = standard error.

Supplementary Table 8: Lead variants from the meta-analysis of genome-wide association studies of pericardial adipose tissue

CHROM	POS	ID	EA	NEA	Nearest gene	Function	P	N	EA AF (UKB)
1	119736529	rs10802081	C	T	WARS2-AS1	ncRNA_intronic	6.61E-16	53081	0.674132
2	12951752	rs2113814	T	C	TRIB2	intergenic	6.31E-21	53080	0.495936
2	72178287	rs908611	T	C	CYP26B1	intergenic	6.92E-09	52569	0.600742
3	49823024	rs11920900	C	G	IP6K1	intronic	2.95E-08	48949	0.316931
5	55860781	rs3936511	G	A	C5orf67	ncRNA_intronic	4.17E-09	53096	0.190317
5	158025983	rs748510	C	T	EBF1	intergenic	2.69E-18	53092	0.237497
19	33795241	rs16967952	A	G	CEBPA-DT	ncRNA_exonic	3.55E-10	51805	0.134691

A p-value based sample size weighted meta-analysis of the UK Biobank genome-wide association study and a previously published GWAS meta-analysis by Chu et al (n = 12,204) was performed using METAL, including up to 53,698 total participants. Lead variants, nearest genes and variant functions are shown. Variant allele frequencies (AF) are based on UK Biobank data only. CHROM = chromosome, POS = position in the GRCh37 build.

Supplementary Table 9: FinnGen participant characteristics

Characteristic	Overall	Females	Males
N	453733	254618	199115
Age at genotyping (mean (SD))	52.92 (17.96)	51.25 (18.15)	55.07 (17.47)
Age at death or end of follow-up (mean (SD))	60.51 (17.97)	58.05 (18.21)	63.67 (17.15)
BMI (mean (SD))	27.31 (5.54)	27.27 (6.04)	27.34 (4.93)
Male sex (%)	199115 (43.9)	0 (0.0)	199115 (100.0)
Type 2 diabetes (%)	79190 (17.7)	35381 (14.1)	43809 (22.3)
Atrial fibrillation or flutter (%)	55853 (19.4)	21088 (12.5)	34765 (29.2)
Heart failure (%)	33250 (7.3)	12476 (4.9)	20774 (10.4)
Coronary heart disease (%)	51098 (11.3)	15028 (5.9)	36070 (18.1)
Stroke (%)	30521 (6.9)	11923 (4.8)	18598 (9.7)

Sample characteristics are shown for 453,733 individuals from data freeze 11. Cardiovascular diseases were defined using a combination of International Classification of Diseases (ICD) codes from specialist inpatient, outpatient and cause-of-death registries, procedure codes, and medication reimbursement codes. Sex, age at genotyping, and body mass index (BMI) were ascertained at study recruitment. Disease-specific outcomes include both prevalent and incident diseases before the end of the follow-up.

Supplementary Table 10: The predictive utility of a polygenic score for pericardial adipose tissue in FinnGen

Model	Outcome	Beta	SE	OR	OR lower 95% CI	OR upper 95% CI	z	P	Cases	Controls
Basic	Stroke	0.02	0.01	1.02	1.01	1.03	2.92	0.0035	30521	408788
Basic	Heart failure	0.05	0.01	1.05	1.04	1.06	7.83	4.79E-15	33250	420483
Basic	Type 2 diabetes	0.06	0.00	1.06	1.05	1.07	13.94	3.57E-44	79190	369038
Basic	Atrial fibrillation or flutter	0.04	0.01	1.04	1.03	1.06	6.85	7.60E-12	55853	231952
Basic	Coronary artery disease	0.03	0.01	1.03	1.02	1.04	6.42	1.37E-10	51098	402635
BMI-adjusted	Stroke	0.02	0.01	1.02	1.01	1.03	2.81	0.0050	30521	408788
BMI-adjusted	Heart failure	0.03	0.01	1.03	1.02	1.05	4.88	1.06E-06	33250	420483
BMI-adjusted	Type 2 diabetes	0.02	0.01	1.02	1.01	1.03	4.49	6.98E-06	79190	369038
BMI-adjusted	Atrial fibrillation or flutter	0.02	0.01	1.02	1.01	1.04	2.75	0.0060	55853	231952
BMI-adjusted	Coronary artery disease	0.03	0.01	1.03	1.02	1.04	4.87	1.10E-06	51098	402635

A polygenic score (PGS) for pericardial adipose tissue (PAT) was constructed using PRS-CS based on summary statistics from the genome-wide association study of PAT in UK Biobank and subsequently applied to 453,733 participants in the FinnGen study. The associations of the PAT PGS with cardiovascular diseases were evaluated using logistic regression models with sex, age at the end of study follow-up or death, genomic principal components 1–5 and the genotyping array as basic covariates. In body mass index (BMI) adjusted models, BMI was included as an additional covariate. Effect estimates are shown per SD increment in PAT PGS. CI = confidence interval, OR = odds ratio.

Supplementary References

1. Deng J, Dong W, Socher R, Li L-J, Li K, Fei-Fei L. ImageNet: A large-scale hierarchical image database. In: 2009 IEEE Conference on Computer Vision and Pattern Recognition. 2009. p. 248–255.

2. He K, Zhang X, Ren S, Sun J. Deep residual learning for image recognition. In: Proceedings of the IEEE conference on computer vision and pattern recognition. 2016. p. 770–778.

3. Weeks EM, Ulirsch JC, Cheng NY, Trippe BL, Fine RS. Leveraging polygenic enrichments of gene features to predict genes underlying complex traits and diseases. *MedRxiv* [Internet]. 2020;Available from: https://www.medrxiv.org/content/10.1101/2020.09.08.20190561.abstract

4. de Leeuw CA, Mooij JM, Heskes T. MAGMA: generalized gene-set analysis of GWAS data. *PLoS Comput Biol* [Internet]. 2015;Available from: https://journals.plos.org/ploscompbiol/article?id=10.1371/journal.pcbi.1004219

5. Willer CJ, Li Y, Abecasis GR. METAL: fast and efficient meta-analysis of genomewide association scans. *Bioinformatics*. 2010;26:2190–2191.

6. Chu AY, Deng X, Fisher VA, Drong A, Zhang Y, Feitosa MF, Liu C-T, Weeks O, Choh AC, Duan Q, Dyer TD, Eicher JD, Guo X, Heard-Costa NL, Kacprowski T, Kent JW Jr, Lange LA, Liu X, Lohman K, Lu L, Mahajan A, O'Connell JR, Parihar A, Peralta JM, Smith AV, Zhang Y, Homuth G, Kissebah AH, Kullberg J, Laqua R, Launer LJ, Nauck M, Olivier M, Peyser PA, Terry JG, Wojczynski MK, Yao J, Bielak LF, Blangero J, Borecki IB, Bowden DW, Carr JJ, Czerwinski SA, Ding J, Friedrich N, Gudnason V, Harris TB, Ingelsson E, Johnson AD, Kardia SLR, Langefeld CD, Lind L, Liu Y, Mitchell BD, Morris AP, Mosley TH Jr, Rotter JI, Shuldiner AR, Towne B, Völzke H, Wallaschofski H, Wilson JG, Allison M, Lindgren CM, Goessling W, Cupples LA, Steinhauser ML, Fox CS. Multiethnic genome-wide meta-analysis of ectopic fat depots identifies loci associated with adipocyte development and differentiation. *Nat Genet*. 2017;49:125–130.

7. Ge T, Chen C-Y, Ni Y, Feng Y-CA, Smoller JW. Polygenic prediction via Bayesian regression and continuous shrinkage priors. *Nat Commun*. 2019;10:1776.

8. Chang CC, Chow CC, Tellier LC, Vattikuti S, Purcell SM, Lee JJ. Second-generation PLINK: rising to the challenge of larger and richer datasets. *Gigascience*. 2015;4:7.

9. Rosenbloom KR, Armstrong J, Barber GP, Casper J, Clawson H, Diekhans M, Dreszer TR, Fujita PA, Guruvadoo L, Haeussler M, Harte RA, Heitner S, Hickey G, Hinrichs AS, Hubley R, Karolchik D, Learned K, Lee BT, Li CH, Miga KH, Nguyen N, Paten B, Raney BJ, Smit AFA, Speir ML, Zweig AS, Haussler D, Kuhn RM, Kent WJ. The UCSC Genome Browser database: 2015 update. *Nucleic Acids Res*. 2015;43:D670–81.

10. R Core Team. R: A language and environment for statistical computing. R Foundation for Statistical Computing, Vienna, Austria [Internet]. 2016. Available from: https://cir.nii.ac.jp/crid/1574231874043578752